JOC Article
pubs.acs.org/joc

Supramolecular Synthons in Noncovalent Synthesis of a Class of Gelators Derived from Simple Organic Salts: Instant Gelation of Organic Fluids at Room Temperature via in Situ Synthesis of the Gelators

Uttam Kumar Das,[†] Darshak R Trivedi,[‡] N. N. Adarsh,[†] and Parthasarathi Dastidar*[,†]

[†]*Department of Organic Chemistry, Indian Association for the Cultivation of Science* (*IACS*), *2A & 2B Raja S C Mullick Road, Jadavpur Kolkata 700032, West Bengal, India.* [‡]*Present address: Department of Chemistry, National Institute of Technology Karnataka* (*NITK*), *Surathkal, Srinivas Nagar, Mangalore 575025, Karnataka, India*

parthod123@rediffmail.com; ocpd@iacs.res.in

Received July 13, 2009

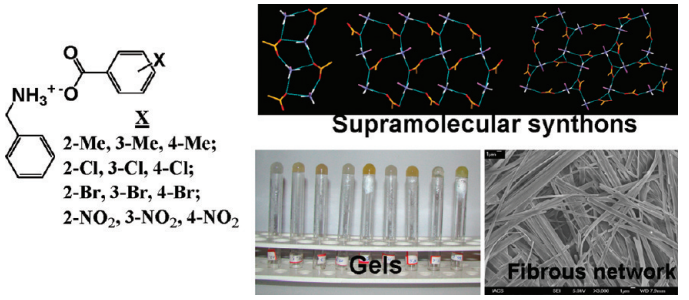

The supramolecular synthon approach has been employed to synthesize noncovalently a series of low molecular mass organic gelators (LMOGs) derived from benzylammonium salts of variously substituted benzoic acids. The majority of the salts (75%) prepared showed interesting gelation properties. Instant gelation of an organic fluid, namely methyl salicylate, was achieved at room temperature by using most of the gelator salts by in situ synthesis of the gelators. Table top rheology and scanning electron microscopy (SEM) were used to characterize the gels. Single crystal X-ray diffraction studies revealed the presence of both 1D and 2D supramolecular synthons. X-ray powder diffraction (XRPD) studies indicated the presence of various crystalline phases in the fibers of the xerogels. By using these data, a structure−property correlation has been attempted and the working hypothesis for designing the gelator has been reinforced.

Introduction

Corey's definition of *synthon*[1] adopted in organic synthesis has been proved to be so general and flexible that it has found its use in noncovalent supramolecular syntdyhesis[2] as well. In supramolecular synthesis, the target molecule is a *supermolecule* (assembly of molecules, e.g., crystal structure) that can be designed and synthesized by using the crystal engineering approach[2,3] wherein "*supramolecular synthons*" as introduced by Desiraju "*are spatial arrangements of intermolecular interactions and play the same focusing role in supramolecular synthesis that conventional synthons do in molecular synthesis*".[2] To illustrate the power of a supramolecular synthon in getting easy access to supramolecular structures with various dimensionalities (0-, 1-, 2-, or 3-dimensional), the frequent occurrence of the COOH dimer hydrogen bonded network (HBN) as a supramolecular synthon may be considered. Thus, introduction of COOH functionality in an aromatic ring results in a 0D network in benzoic acid,[4] a 1D linear and zigzag network in terephthalic acid[5] and isophthalic acid,[6] respectively, a 2D honeycomb network in trimesic acid,[7] and a 3D diamond network in adamentanoid tetracarboxylic acid[8] (Scheme 1).

(1) Corey, E. J. *Pure Appl. Chem.* **1967**, *14*, 19.
(2) (a) Desiraju, G. R. *Angew. Chem., Int. Ed.* **1995**, *34*, 2311. (b) Thalladi, V. R.; Goud, B. S.; Hoy, V. J.; Allen, F. H.; Howard, J. A. K.; Desiraju, G. R. *Chem. Commun.* **1996**, 401.
(3) (a) Desiraju, G. R. *Angew. Chem., Int. Ed.* **2007**, *46*, 8342. (b) Desiraju, G. R. *J. Mol. Struct.* **2003**, *656*, 5.
(4) Bruno, G.; Randaccio, L. *Acta Crystallogr.* **1980**, *B36*, 1711.
(5) Bailey, M.; Brown, C. J. *Acta Crystallogr.* **1967**, *22*, 387.
(6) (a) Alcala, R.; Carrera, S. M. *Acta Crystallogr., Sect. B* **1972**, *28*, 1671. (b) Derissen, J. L. *Acta Crystallogr., Sect. A* **1974**, *30*, 2764.
(7) Duchamp, D. J.; Marsh, R. E. *Acta Crystallogr.* **1969**, *B25*, 5.
(8) Ermer, O. *J. Am. Chem. Soc.* **1988**, *110*, 3747.

DOI: 10.1021/jo901463k Published on Web 08/13/2009

SCHEME 1. Various Dimensionalities in the Supramolecular Structures by Exploiting COOH Dimer Synthon[a]

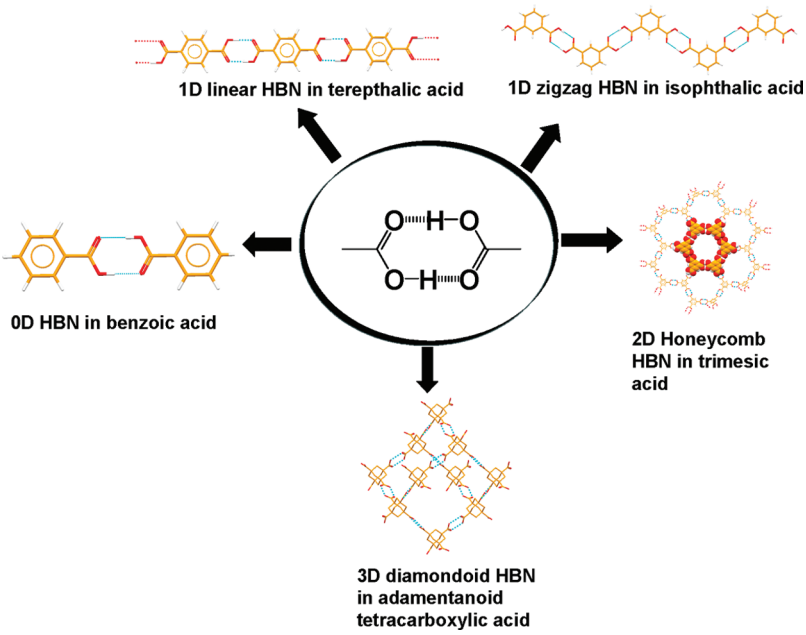

[a]The figures are generated by retrieving the crystallographic information files (CIFs) deposited in the Cambridge Structural Database (CSD).

Thus, it is important to identify supramolecular synthons that are robust enough to ensure generality and predictability in the supramolecular structures and consequently properties. Indeed, there are plenty of reports wherein supramolecular synthons have been exploited to generate desired supramolecular structures.[9] In this context, a low molecular mass organic gelator (LMOG)[10] is an attractive supramolecular target. Typically, when a hot solution containing LMOG at a critical concentration (minimum gelator concentration or MGC) is cooled below a critical temperature (sol−gel transition), the whole volume of liquid displays a solid-like behavior. The solid-like viscoelastic material thus obtained is a gel. Due to their various potential applications such as in sensors,[11] electrooptics/photonics,[12] structure-directing agents,[13] cosmetics,[14] conservation of arts,[15] drug delivery,[16] and biomedical applications[17] etc., research on LMOGs has been intensified in recent years.

However, designing a gelator molecule is still a daunting task. It is understood that during gel formation, the gelator molecules form self-assembled fibrilar networks (SAFINs)[18] that by some means manage to self-assemble into complicated 3D SAFINs within which the solvent molecules are

(9) (a) Aakeroy, C. B.; Scott, B. M. T.; Smith, M. M.; Urbina, J. F.; Desper, J. *Inorg. Chem.* **2009**, *48*, 4052. (b) Bhatt, P. M.; Azim, Y.; Thakur, T. S.; Desiraju, G. R. *Cryst. Growth Des.* **2009**, *9*, 951. (c) Banerjee, R.; Saha, B. K.; Desiraju, G. R. *CrystEngComm* **2006**, *8*, 680. (d) Reddy, L. S.; Babu, N. J.; Nangia, A. *Chem. Commun.* **2006**, *13*, 1369. (e) Aakeroy, C. B.; Desper, J.; Urbina, J. F. *Chem. Commun.* **2005**, *22*, 2820. (f) Turner, D. R.; Smith, B.; Goeta, A. E.; Evans, I. R.; Tocher, D. A.; Howard, J. A. K.; Steed, J. W. *CrystEngComm* **2004**, *6*, 633. (g) Allen, F. H.; Hoy, V. J.; Howard, J. A. K.; Thalladi, V. R.; Desiraju, G. R.; Wilson, C. C.; McIntyre, G. J. *J. Am. Chem. Soc.* **1997**, *119*, 3477. (h) Reddy, D. S.; Ovchinnikov, Y. E.; Shishkin, O. V.; Struchkov, Y. T.; Desiraju, G. R. *J. Am. Chem. Soc.* **1996**, *118*, 4058. (i) Kumar, D. K.; Das, A.; Dastidar, P. *Cryst. Growth Des.* **2006**, *6*, 216. (j) Kohmoto, S.; Kuroda, Y.; Someya, Y.; Kishikawa, K.; Masu, H.; Yamaguchi, K.; Azumaya, I. *Cryst. Growth Des.* **2009**, *9* , 3457. (k) Thaimattam, R.; Krishnamohan Sharma, C. V.; Clearfield, A.; Desiraju, G. R. *Cryst. Growth Des.* **2001**, *1*, 103.

(10) (a) Dastidar, P. *Chem. Soc. Rev.* **2008**, *37*, 2699. (b) George, M.; Weiss, R. G. *Acc. Chem. Res.* **2006**, *39*, 489. (c) Sangeetha, N. M.; Maitra, U. *Chem. Soc. Rev.* **2005**, *34*, 821. (d) Gronwald, O.; Snip, E.; Shinkai, S. *Curr. Opin. Colloid Interface Sci.* **2002**, *7*, 148. (e) Terech, P.; Weiss, R. G. *Chem. Rev.* **1997**, *97*, 3133. (f) Abdallah, D. J.; Weiss, R. G. *Adv. Mater.* **2000**, *12*, 1237. (g) Bag, B. G.; Maity, G. C.; Dinda, S. K. *Org. Lett.* **2006**, *8*, 5457. (h) Pal, A.; Hajra, B.; Sen, S.; Aswal, V. K.; Bhattacharya, S. *J. Mater. Chem.* **2009**, *19*, 4325. (i) Terech, P.; Dourdain, S.; Maitra, U.; Bhat, S. *J. Phys. Chem. B* **2009**, *113*, 4619. (j) Palui, G.; Banerjee, A. *J. Phys. Chem. B* **2008**, *112*, 10107. (k) Vijayakumar, C.; Praveen, V. K.; Ajayaghosh, A. *Adv. Mater.* **2009**, *21*, 2059. (l) Dutta, S.; Shome, A.; Debnath, S.; Das, P. K. *Soft Matter* **2009**, *5*, 1607. (m) Pal, A.; Chhikara, B. S.; Govindaraj, A.; Bhattacharya, S.; Rao, C. N. R. *J. Mater. Chem.* **2008**, *18*, 2593. (n) Ghosh, R.; Chakraborty, A.; Maiti, D. K.; Puranik, V. G. *Org. Lett.* **2006**, *8*, 1061. (o) Díaz, D. D.; Cid, J. J.; Vázquez, P.; Torres, T. *Chem.—Eur. J.* **2008**, *14*, 9273. (p) Dawn, A.; Fujita, N.; Haraguchi, S.; Sada, K.; Shinkai, S. *Chem. Commun.* **2009**, 2100. (q) Suzuki, M; Hanabusa, K. *Chem. Soc. Rev.* **2009**, *38*, 967. (r) Piepenbrock, M.-O. M.; Lloyd, G. O.; Clarke, N.; Steed, J. W. *Chem. Commun.* **2008**, 2644. (s) Hirst, A. R.; Miravet, J. E.; Escuder, B.; Noirez, L.; Castelletto, V.; Hamley, I. W.; Smith, D. K. *Chem.—Eur. J.* **2009**, *15*, 372. (t) Placin, F.; Colomès, M.; Desvergne, J.-P. *Tetrahedron Lett.* **1997**, *38*, 2665. (u) Hopf, H.; Greiving, H.; Bouas-Laurent, H.; Desvergne, J. P. *Eur. J. Org. Chem.* **2009**, 1868. (v) Huang, X.; Raghavan, S. R.; Terech, P.; Weiss, R. G. *J. Am. Chem. Soc.* **2006**, *128*, 15341. (w) Baddeley, C.; Yan, Z, Q.; King, G.; Woodward, P. M.; Badjic, J. D. *J. Org. Chem.* **2007**, *72*, 7270. (x) Raghavan, S. R.; Cipriano, B. H. In *Molecular Gels. Materials with Self-Assembled Fibrillar Networks*; Weiss, G., Terech, P., Eds.; Springer: Dordrecht, The Netherlands, 2005; Chapter 8, p 241. (y) Menger, F. M.; Caran, K. L. *J. Am. Chem. Soc.* **2000**, *122*, 11679. (z) Suzuki, M.; Nakajima, Y.; Yumoto, M.; Kimura, M.; Hirai, H.; Hanabusa, K. *Org. Biomol. Chem.* **2004**, *2*, 1155.

(11) (a) Murata, K.; Aoki, M.; Nishi, T.; Ikeda, A.; Shinkai, S. *J. Chem. Soc., Chem. Commun.* **1991**, 1715. (b) de Jong, J. J. D.; Lucas, L. N.; Kellogg, R. M.; van. Esch, J. H.; Feringa, B. L. *Science* **2004**, *304*, 278.

(12) (a) Kato, T. *Science* **2002**, *295*, 2414. (b) Ajayaghosh, A.; Praveen, V. K.; Vijayakumar, C.; George, S. J. *Angew. Chem., Int. Ed.* **2007**, *46*, 6260.

(13) (a) van Bommel, K. J. C.; Friggeri, A.; Shinkai, S. *Angew. Chem., Int. Ed.* **2003**, *42*, 980. (b) Basit, H.; Pal, A.; Sen, S.; Bhattacharya, S. *Chem.−Eur. J.* **2008**, *14*, 6534. (c) Ray, S.; Das, A. K.; Banerjee, A. *Chem. Commun.* **2006**, 2816. (d) Gundiah, G.; Mukhopadhyay, S.; Tumkurkar, U. G.; Govindaraj, A.; Maitra, U.; Rao, C. N. R. *J. Mater. Chem.* **2003**, *13*, 2118.

(14) Wynne, A.; Whitefield, M.; Dixon, A. J.; Anderson, S. *J. Dermatol. Treat.* **2002**, *13*, 61.

(15) Carretti, E.; Dei, L. In *Molecular Gels. Materials with Self-Assembled Fibrillar Networks*; Weiss, G., Terech, P., Eds.; Springer: Dordrecht, The Netherlands, 2005; Chapter 27, p 929.

(16) Lee, K. Y.; Mooney, D. *J. Chem. Rev.* **2001**, *101*, 1869.

(17) Yang, Z.; Liang, G.; Wang, L.; Xu, B. *J. Am. Chem. Soc.* **2006**, *128*, 3038.

(18) Weiss, R. G.; Terech, P., Eds. *Molecular Gels. Materials with Self-Assembled Fibrillar Networks*; Springer: Dordrecht, The Netherlands, 2005.

SCHEME 2

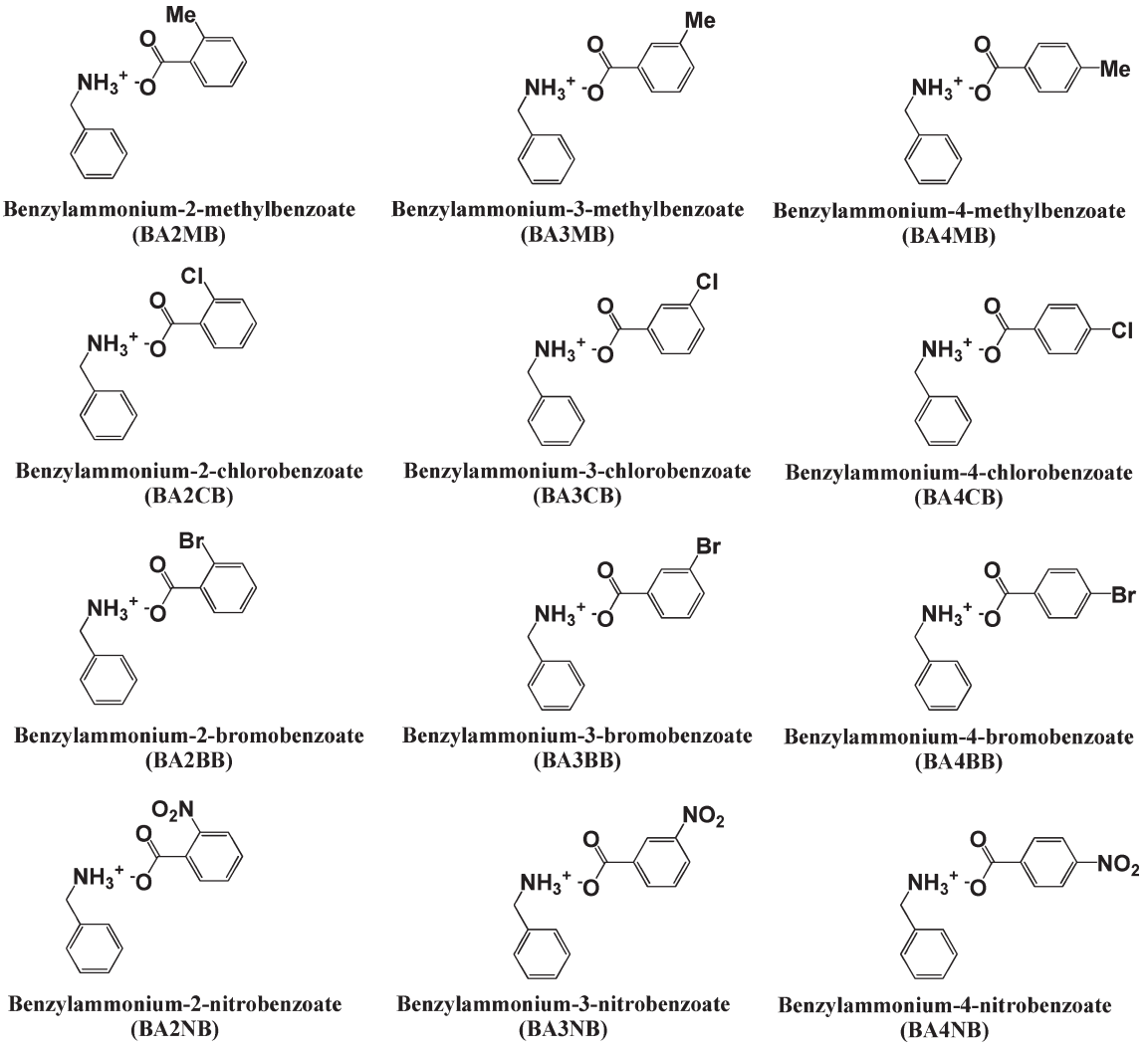

immobilized due to capillary force resulting in gel formation. Wide structural diversities of the molecules known to act as LMOGs and lack of molecular level understanding of the gel formation mechanism make it difficult to pinpoint a particular strategy to achieve a rational design of gelators.

A closer look at the SAFINs by using different optical, electron, and force microscopy reveals various morphological features of which highly branched and/or entangled 1D fiber is the most noteworthy. It is, therefore, reasonable to believe that there must be some anisotropic interactions of the gelator molecules that allow growth in one direction and lack of such interactions in the other two dimensions prevents lateral growth resulting in 1D fibers. Thus a molecule having self-complementary, reasonably strong and directional hydrogen bonding site(s) is expected to grow as a 1D fiber under suitable conditions, which may favor SAFIN formation resulting in a gel.

To support this hypothesis, there was only one report[19] that concluded that the 1D network promoted gelation whereas 2D and 3D networks either produced weak gel or no gelation at all until we demonstrated[20] most explicitly with a number of organic salt based compounds that the hypothesis indeed was based on a logical foundation. Thus, it is worth identifying a supramolecular synthon that would promote the 1D network in the target supermolecule as a potential gelling agent.

We have been mainly focusing our attention on organic salt based compounds as potential gelators for the following reasons: (a) organic salt formation is probably the easiest

(19) Luboradzki, R.; Gronwald, O.; Ikeda, M.; Shinkai, S.; Reinhoudt, D. N. *Tetrahedron* **2000**, *56*, 9595.

(20) (a) Adarsh, N. N.; Kumar, D. K.; Dastidar, P. *Tetrahedron* **2007**, *63*, 7386. (b) Ballabh, A.; Adalder, T. K.; Dastidar, P. *Cryst. Growth Des.* **2008**, *8*, 4144. (c) Trivedi, D. R.; Ballabh, A.; Dastidar, P.; Ganguly, B. *Chem.—Eur. J.* **2004**, *10*, 5311. (d) Sahoo, P.; Kumar, D. K.; Trivedi, D. R.; Dastidar, P. *Tetrahedron Lett.* **2008**, *49*, 3052. (e) Trivedi, D. R.; Dastidar, P. *Chem. Mater.* **2006**, *18*, 1470. (f) Kumar, D. K.; Jose, D. A.; Das, A.; Dastidar, P. *Chem. Commun.* **2005**, 4059. (g) Trivedi, D. R.; Ballabh, A.; Dastidar, P. *J. Mater. Chem.* **2005**, *15*, 2606. (h) Trivedi, D. R.; Ballabh, A.; Dastidar, P. *Cryst. Growth Des.* **2006**, *6*, 763. (i) Ballabh, A.; Trivedi, D. R.; Dastidar, P. *Org. Lett.* **2006**, *8*, 1271. (j) Trivedi, D. R.; Dastidar, P. *Cryst. Growth Des.* **2006**, *6*, 1022. (k) Trivedi, D. R.; Dastidar, P. *Cryst. Growth Des.* **2006**, *6*, 2114. (l) Ballabh, A.; Trivedi, D. R.; Dastidar, P. *Chem. Mater.* **2003**, *15*, 2136. (m) Kumar, D. K.; Jose, D. A.; Dastidar, P.; Das, A. *Langmuir* **2004**, *20*, 10413. (n) Kumar, D. K.; Jose, D. A.; Dastidar, P.; Das, A. *Chem. Mater.* **2004**, *16*, 2332. (o) Trivedi, D. R.; Ballabh, A.; Dastidar, P. *Chem. Mater.* **2003**, *15*, 3971. (p) Ballabh, A.; Trivedi, D. R.; Dastidar, P. *Chem. Mater.* **2003**, *15*, 2136.

reaction to carry out in chemistry (within a short span, it is possible to prepare a large number of salts with quantitative or near-quantitative yield, which can be screened for gelation behavior), (b) the charge-assisted hydrogen bonds present in organic salts are stronger compared to normal hydrogen bonds (10−65 and 40−190 kJ mol^{-1} for normal and charge assisted hydrogen bonds, respectively) thereby making the product more robust, which is often a criterion for real-life applications, and (c) the commercial availability of various acids and amines and their virtually infinite number of combinations opens up an opportunity to explore a combinatorial library approach in discovering new LMOGs.[21] Thus, the noncovalent approach is definitely advantageous over the time-consuming covalent approach (typical multistep organic synthesis), which often leads to frustration in the quest for new LMOGs.

Among the supramolecular synthons that we identified and exploited in designing a large number of LMOGs,[10a] the primary ammonium monocarboxylate (**PAM**) synthon is particularly interesting. **PAM** salts frequently display 1D HBN along with the occasional 2D HBNs. Since both 1D HBN is important in gelation and 2D HBN can also promote weak gelation, it is worthwhile to scan some selected class of **PAM** salts for gelation properties. Toward this goal, we have recently exploited the **PAM** synthon in discovering a new class of gelling agents.[21b]

Herein, we report the synthesis, characterization, and gelation studies of a new class of gelling agents derived from various **PAM** salts from differently substituted benzoic acids and benzylamine (Scheme 2). Interestingly, in situ synthesis of most of the gelator salts enabled instant gelation of a targeted organic fluid, namely, methyl salicylate, at room temperature.[10y] Supramolecular synthons present in some of the gelator and nongelator salts have been identified from single crystal X-ray diffraction. Structure−property correlation based on single crystal and powder X-ray diffraction data is also attempted.

Results and Discussion

Synthesis, Gelation, and Characterization. All the salts were prepared by reacting the corresponding benzoic acid and benzylamine in 1:1 molar ratio in MeOH at ambient condition (see the Experimental Section). FT-IR data clearly indicated the salt formation (vide infra). The salts were then scanned for gelation properties with a few prototype solvents which included both polar and nonpolar solvents (Table 1). In a typical gelation experiment, a known amount of salt was dissolved in a known volume of solvent and heated. If the whole volume of the liquid turned into solid-like material (checked by tube inversion) upon cooling, it was termed a gel. The majority of the salts (75%) prepared herein were able to gel various solvents in a thermoreversible manner; both the polar and nonpolar solvents could be gelled with remarkable efficiency (minimum gelator concentration, MGC = 1.2−3.3 wt %, w/v) and stability (gel−sol dissociation temperature, T_{gel} = 50−120 °C) (Table 1). Substituents

TABLE 1. Gelation Data[a]

		BA2MB		BA3MB		BA4MB		BA2CB		BA3CB		BA4CB		BA2BB		BA3BB		BA4BB		BA2NB		BA3NB		BA4NB	
sr. no	solvent	MGC/ wt %	T_{gel}/ °C	MGC/ wt %	T_{gel}/ °C	MGC/ wt %	T_{gel}/ °C	MGC/ wt %	T_{gel}/ °C	MGC/ wt %	T_{gel}/ °C	MGC/ wt %	T_{gel}/ °C	MGC/ wt %	T_{gel}/ °C	MGC/ wt %	T_{gel}/ °C	MGC/ wt %	T_{gel}/ °C	MGC/ wt %	T_{gel}/ °C	MGC/ wt %	T_{gel}/ °C	MGC/ wt %	T_{gel}/ °C
1	acetonitrile	1.8	50	FC		2.5	74	3.3	74	PC		2.3	76	2.5	84	NC		PC		L		FC		PC	
2	*o*-xylene	1.8	78	FN		GP		2.8	96	FC		GF		2.2	96	GF		GP		FP		FC		FP	
3	*m*-xylene	1.2	68	GP		GP		2.5	100	GP		2.3	84	2.0	100	GP		GP		FP		FC		PC	
4	*p*-xylene	1.3	70	GP		GP		3.3	104	GP		2.3	85	1.6	94	FC		GP		FP		FC		PC	
5	chlorobenzene	2.5	66	2.5	64	GP		2.5	86	FP		2.3	72	2.5	84	GP		3.3	86	NC		4	120		
6	1,2-dichlorobenzene	2.5	68	2.0	66	FC		2.2	88	NC		2.3	75	2.0	80	GF		3.3	82	NC		3.3	112	GP	
7	nitrobenzene	2.0	60	L		FC		2.0	62	PC		2.0	72	2.5	74	GP		2.0	56	L		0.8	84	2.2	84
8	toluene			WP		FP				GP		2.3	68	1.6	90	GF		GP		FP		FC		GP	
9	mesitylene	1.5	76	GP		FP		2.5	106	FP		GF		1.5	98	GP		GP		FP		FC		GP	
10	methylsalicylate	1.8	60	2.85	64	2.22	80	2.2	82	FN		GF		1.5	68	L		2.5	72	L		3.3	96	PC	
11	*n*-hexane	L		L		NC		L		I		L		L		I		NC		PC		FC		P	
12	DMF	L		L		L		L		L		L		L		L		L		L		L		L	
13	DMSO	L		L		L		L		L		L		L		L		L		L		L		L	
14	water	L		L		L		L		L		L		L		L		PC		L		L		L	
15	methanol	L		L		L		L		L		L		L		L		L		FC		L		PC	
16	petrol	PC		NC		NC		FN		L		FN		L		ND		NC		ND		NC		PC	

[a]In addition of co-solvent ethanol L = liquid, FC = fibrous crystal, FN = fibrous network, GP = gelatinous precipitate, WP = white precipitate, FP = fibrous precipitate, PC = plate like crystal, NC = needle shaped crystal, GF = gelatinous fibrous, P = precipitate, I = insoluble, and ND = not done.

(21) (a) Dastidar, P.; Okabe, S.; Nakano, K.; Iida, K.; Miyata, M.; Tohnai, N.; Shibayama, M. *Chem. Mater.* **2005**, *17*, 741. (b) Ballabh, A.; Trivedi, D. R.; Dastidar, P. *Chem. Mater.* **2006**, *18*, 3795. (c) Sahoo, P.; Adarsh, N. N.; Chacko, G. E.; Raghavan, S. R.; Puranik, V. G.; Dastidar, P. *Langmuir* **2009**, *25*, 8742. (d) Nakano, K.; Hishikawa, Y.; Sada, K.; Miyata, M.; Hanabusa, K. *Chem. Lett.* **2000**, 1170.

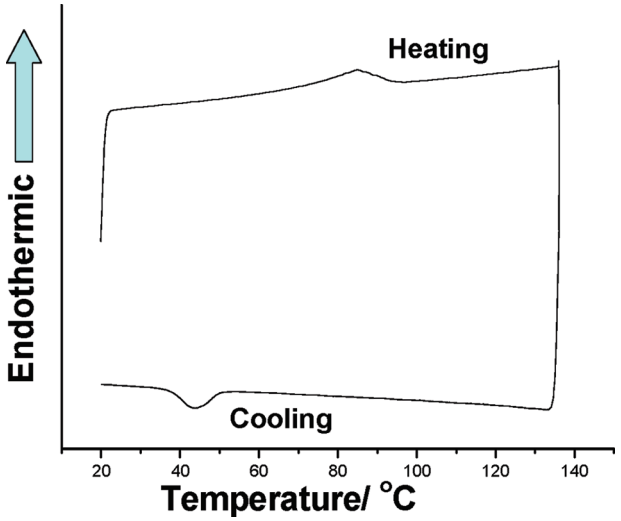

FIGURE 1. DSC trace of a ~4.0 wt % methyl salicylate gel of **BA2CB**.

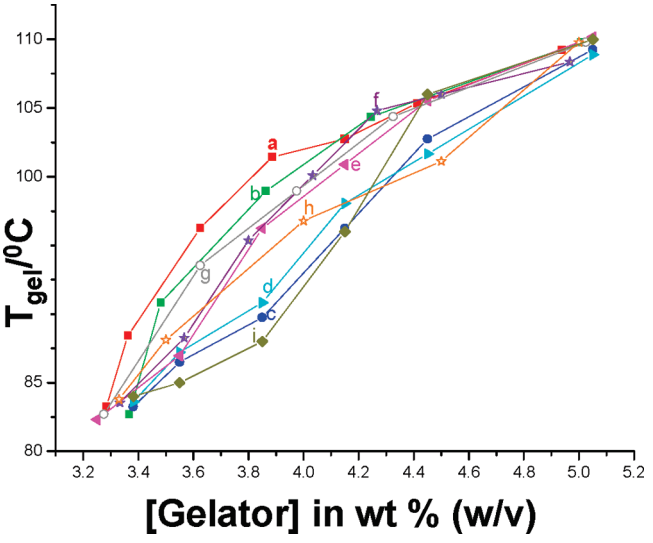

FIGURE 2. T_{gel} vs. [gelator] plot: (a) **BA2MB** (in MS); (b) **BA3MB** (in MS); (c) **BA4MB** (in MS); (d) **BA2CB**(in MS); (e) **BA4CB** (in NB); (f) **BA2BB** (in MS); (g) **BA4BB** (in MS); (h) **BA3NB** (in MS); (i) **BA4NB** (in NB) [MS = methyl salicylate; NB = nitrobenzene].

on the anionic moiety of the salts seemed to have a profound effect on the gelation ability: while 2-substituted salts were found to be the most versatile gelators (except **BA2NB**), 3- and 4-substituted ones were not so efficient and versatile (except **BA4CB**). It is worth noting that substituents at the 4 position resulted in a maximum number of gelators (100%) followed by substituents at 2 (75%) and 3 (50%) positions.

Differential scanning calorimetry (DSC) was recorded on a few gels to see the thermoreversibility of the gels. Figure 1 depicts DSC trace of a ~4.0 wt % methyl salicylate gel of **BA2CB** gelator. While it is clear that the gelation is thermoreversible, the gel−sol transition occurs over a broad temperature range making it difficult to assess the enthalpy associated with the process. To obtain an approximate assessment of enthalpy involved in gel−sol transition, the gels were further characterized by table top rheology.[10w] T_{gel} for each gelator in a given solvent (methyl salicylate or nitrobenzene) was measured by the dropping ball method (see the Experimental Section) at various gelator concentrations. T_{gel} vs. [gelator] plot of all the gelators showed a steady increase in T_{gel} with the increase in concentration (Figure 2), which may be attributed to the dissolution of the gel network indicating that the self-assembly in the gel state is driven by strong intermolecular interactions such as hydrogen bonding. Interestingly, when the semilog of the mole fraction of each gelator at each concentration was plotted against $1/T_{gel}$ K^{-1}, nice linear plots were obtained that represented the Schroeder−van Laar equation (eq 1, Figure 3).[10x]

$$\ln[\text{gelator}] = -(\Delta H_m/RT_{gel}) + \text{constant} \qquad (1)$$

wherein ΔH_m and T_{gel} are the enthalpy of melting and transition temperature of gel−sol transition, respectively.

This means that the gel-to-sol transition can be considered a first order transition assuming that the gel melts into an ideal solution and a known amount of gelator is involved in the transition. From the plots, the enthalpy ΔH_m was calculated to be within the range of 21−71 kJ/mol.

Gel formation at ambient condition without the heating and cooling process has an important technological advantage in real-life applications. Interestingly, all the gelators (except **BA4BBb**, **BA4CB**, and **BA4NB**) showed instant gelation abilities by synthesizing the gelator in situ.[10y] In a typical experiment, a known amount of the acid was dissolved in methyl salicylate (0.5 mL in a 10 mm × 100 mm test tube) by sonication; to this solution, an equivalent amount of benzylamine was added (the amount of the acid and benzylamine was calculated in such a way that the final concentration of the gelator become 4 wt %). The upper part of the solution immediately turned gel-like. Upon hand-shaking the mixture to homogeneity, the whole volume of the liquid was gelled within ~10s.

To see the morphological features of the gel fibers, a dried, collapsed network of the gel fibers (xerogels) was prepared on the SEM stubs. SEM micrographs were recorded for methyl salicylate xerogels derived from all the gelators (Figure 4). In most of the cases, the gel network appeared to be made up of 1D fibers of varying length and thickness. While in many cases, the 1D fibers formed an entangled network (**BA2MB**, **BA3MB**, **BA4MB**, **BA2CB**, and **BA4BB**), in a few cases, they remained highly aligned (**BA4CB**, **BA2BB**, and **BA4NB**). Interestingly, in the case of **BA4CB**, the highly aligned fibers appeared to be made up of colloidal particles whereas the fibers in **BA2BB** were made up of a bundle of fibers. The solvent molecules were understandably immobilized in these networks to form gel.

Supramolecular Synthons in the Present Study. The present work was undertaken with the aim of reinforcing the proof of the working hypothesis that 1D HBN facilitates SAFIN formation (and consequently gel in suitable conditions) whereas 2D and 3D HBNs produce either weak gel or no gelation at all. The chances of being a gelator among **PAM** salts remain high since these salts display mainly 1D with occasional 2D synthons. The fact that about 75% of the **PAM** salts studied herein were gelators clearly indicated the significance of the working hypothesis as discussed above. Thus, it has become essential to study the HBN of the salts in the corresponding single crystal structures. Attempts to crystallize all the salts resulted in good quality single crystals

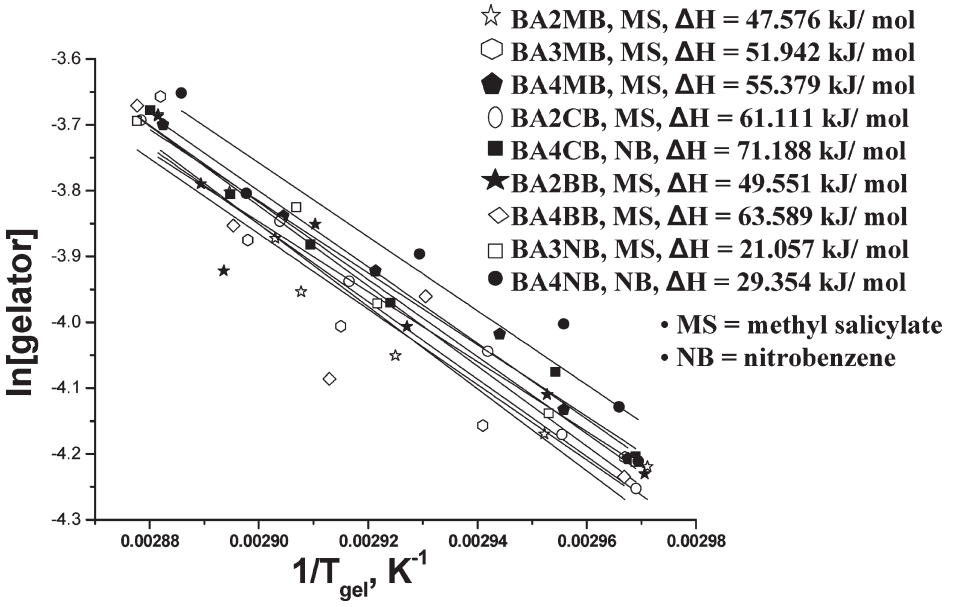

FIGURE 3. Semilog plot of the mole fraction of the gelators against $1/T$.

of seven out of twelve salts studied herein (Table S1, Supporting Information). The following section will focus on the supramolecular synthons present in these structures and its implication on gelation behavior. Already reported single crystal structure of the salt **BA4MB** are also discussed in this context.[22]

CSD analyses of the single crystal structures of various salts derived from aromatic acids and monoaromatic substituted methyl amines revealed the existence of four types of supramolecular synthons (Scheme 3).[23] The most frequent one is the 1D synthon wherein two ammonium and two carboxylate anions form a 10-membered hydrogen bonded ring that propagates in 1D (synthon W). The other 1D synthon (synthon X) is comprised of alternating 12- and 8-membered hydrogen bonded rings. 2D synthons are comprised of 8- and 24-membered (synthon Y) and 16-membered (synthon Z) hydrogen bonded rings (Scheme 3). The occurrence of synthons X, Y, and Z is significantly less than that of synthon W. The main noncovalent interaction in these synthons is the $N^+-H\cdots O^-$ type of charge assisted hydrogen bonding.

The crystal structures of the salts studied herein may be categorized into two classes based on the dimensionality of the supramolecular synthons. While four salts (**BA3MB**, **BA4MB**, **BA2NB**, **BA3NB**) displayed a 1D supramolecular synthon, the other salts (**BA3CB**, **BA4CB**, **BA3BB**, **BA4NB**) showed a 2D supramolecular synthon. Three of the four salts belonging to the former category displayed the centrosymmetric monoclinic space group $P2_1/c$ whereas the salt **BA3NB** crystallized in the noncentrosymmetric orthorhombic space group $P2_12_12_1$. An illustration of various structural features of these salts is given in Figure 5.

The C−O distances of the carboxylate moiety found in the range of 1.234(2)−1.273(3) Å clearly indicated proton transfer or salt formation in these structures. The absence of the COOH band in FT-IR of the parent acid (1678−1693 cm^{-1}) and the appearance of the COO^- band (1624−1632 cm^{-1}) in the salts also confirmed salt formation. Crystal structures of these salts are mainly driven by the charge assisted $N^+-H\cdots O^-$ type of hydrogen bonding [$N^+\cdots O^-$ = 2.6976(14)−2.855(7) Å;$\angle N^+-H\cdots O^-$ = 150.9(18)−177.0(18)°; the details of the hydrogen bonding parameters are given in the Supporting Information]. Interestingly, three of the four salts (**BA3MB**, **BA4MB**, and **BA3NB**) belonging to this category were gelators displaying a 1D supramolecular synthon identical to synthon W whereas the other salt, namely **BA2NB**, turned out to be a nongelator and showed synthon X (Scheme 3). The 1D hydrogen bonded chains in these structures are packed in parallel fashion. $\pi-\pi$ interactions (3.617 Å) involving the 2-nitrobenzoate moieties of the neighboring chains could be observed in the salt **BA2NB** (Figure 5).

In the other category, the majority of the salts crystallized in the centrosymmetric monoclinic space group $P2_1/c$ whereas the salt **BA4NB** displayed the centrosymmetric orthorhombic space group *Pbca*. A polymorphic form (space group $P2_1/c$) of the salt **BA4NB** is also known.[22] Figure 6 depicts the various structural aspects in these salts. Evidence of proton transfer (salt formation) is quite clear from the C−O bond distances of the carboxylate moiety [1.236(6)−1.265(5)Å] and the absence of the COOH band (1678−1693 cm^{-1}) of the parent acids and the presence of the COO^- band (1632−1636 cm^{-1}) in FT-IR. The self-assembly of the ion pairs in these structures is mainly governed by a charge assisted $N^+-H\cdots O^-$ type of hydrogen bonding [$N^+\cdots O^-$ = 2.745(3)−2.883(7) Å; $\angle N^+-H\cdots O^-$ = 146−180°; see the Supporting Information for more details]. Both the 2D synthons Y and Z observed for the salts of aromatic acids and monoaromatic substituted methyl amines (Scheme 3) are absent in these structures. Instead, three different types of 2D hydrogen bonded networks are found. The 2D HBN present in the salt **BA4CB** is constituted of 16-membered rings involving 3 ion pairs whereas

(22) Parshad, H.; Frydenvang, K.; Liljefors, T.; Sorensen, H. O.; Larsen, C. *Int. J. Pharm.* **2004**, *269*, 157.

(23) CSD version 5.30 (November 2008)—search fragment comprised of aromatic carboxylate and monoaromatic methyl ammonium moiety resulting in 80 relevant hits of which 71 hits displayed synthon W followed by synthon X (5 hits), synthon Y (3 hit), and synthon Z (1 hits).

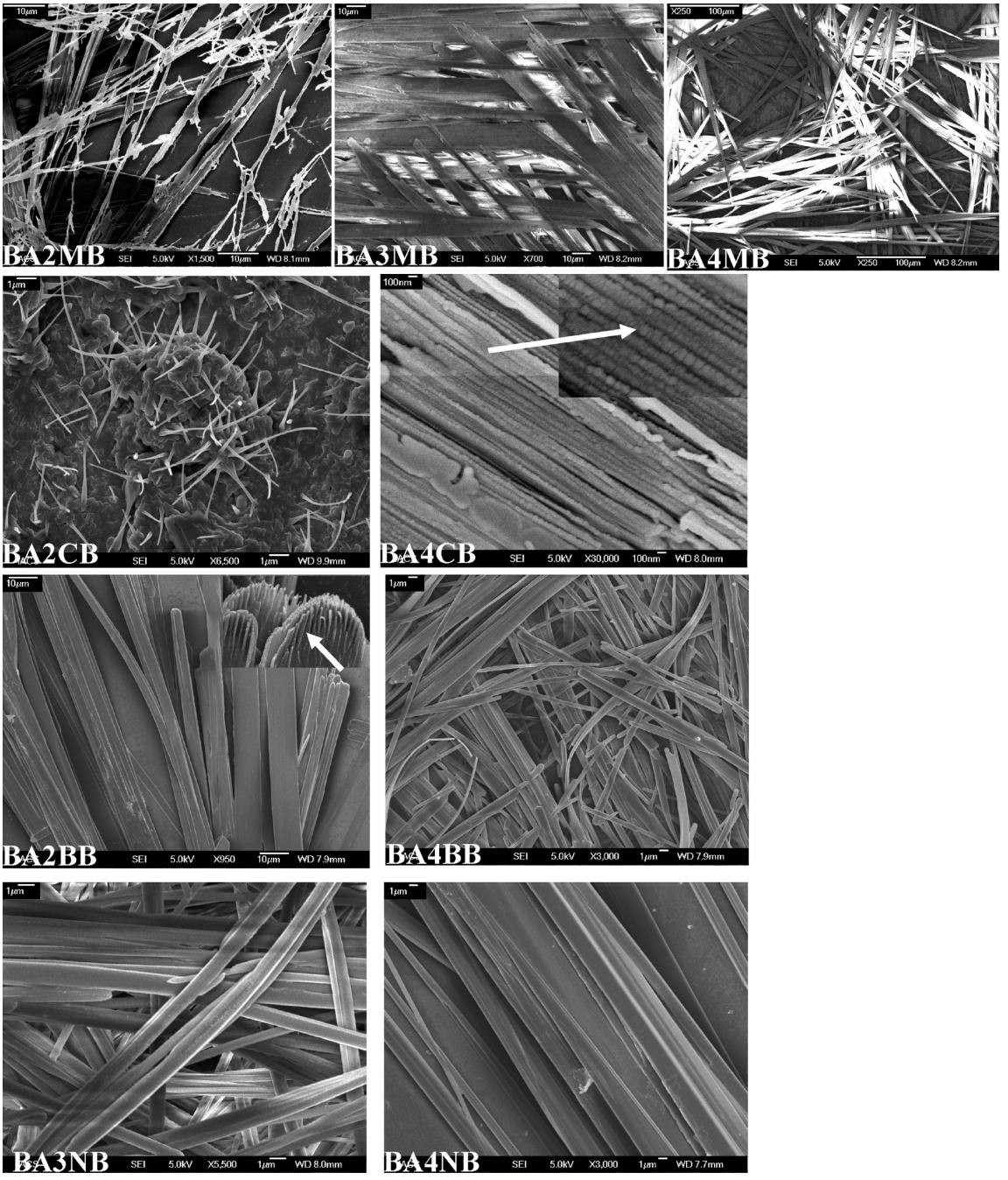

FIGURE 4. SEM micrographs of all the xerogels (methyl salicylate).

20- and 8-membered rings involving 4 and 2 ion pairs, respectively, are the main characteristics of the 2D HBN in the salt **BA4NB**. Both **BA3CB** and **BA3BB**, on the other hand, displayed identical 2D HBN wherein 14- and 8-membered rings involving 4 and 2 ion pairs, respectively, are present (Figure 6). Interestingly, two of the salts, namely **BA4CB** and **BA4NB**, that showed two different 2D HBNs are gelators whereas the nongelator salts (**BA3CB** and **BA3BB**) displayed identical 2D HBNs.

To determine the structure of the gel fibers in the xerogels, X-ray powder diffraction (XRPD) patterns of the xerogels were compared with the simulated and bulk XRPDs following a method originally described by Weiss et al.[24] While the simulated and bulk XRPDs of the salts (**BA3MB**, **BA4MB**, **BA4CB**, **BA3NB**, and **BA4NB**) were found nearly superimposable, none of the XRPD patterns of the corresponding xerogels matched well with that of the simulated and bulk XRPDs (Figure 7).

This means that the single crystal structures of the salts concerned truly represent the bulk materials whereas the corresponding xerogels contain different crystalline phases. Considering the fact that during the solvent removal stage of xerogel formation the gel fibers as well as the soluble gelator undergo a crystallization process, formation of various other crystalline phases (morphs) cannot be ruled out.

(24) Ostuni, E.; Kamaras, P.; Weiss, R. G. *Angew. Chem., Int. Ed. Engl.* **1996**, *35*, 1324.

SCHEME 3

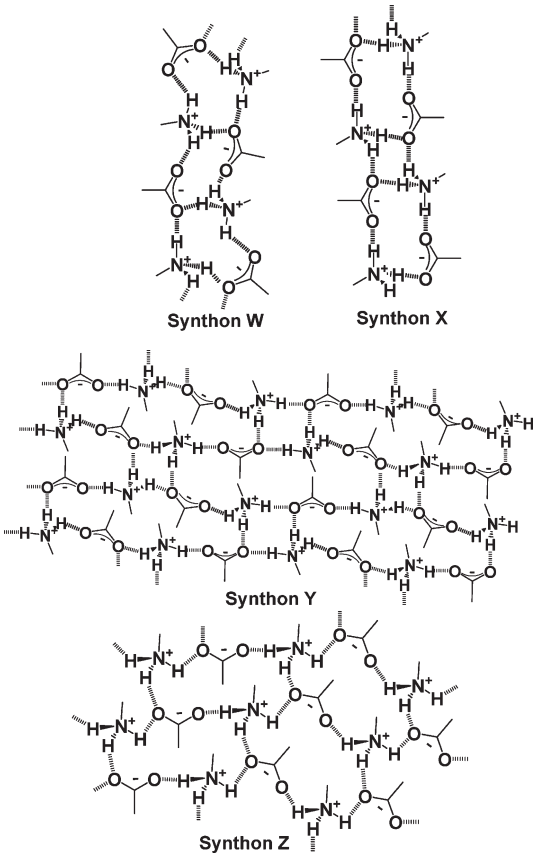

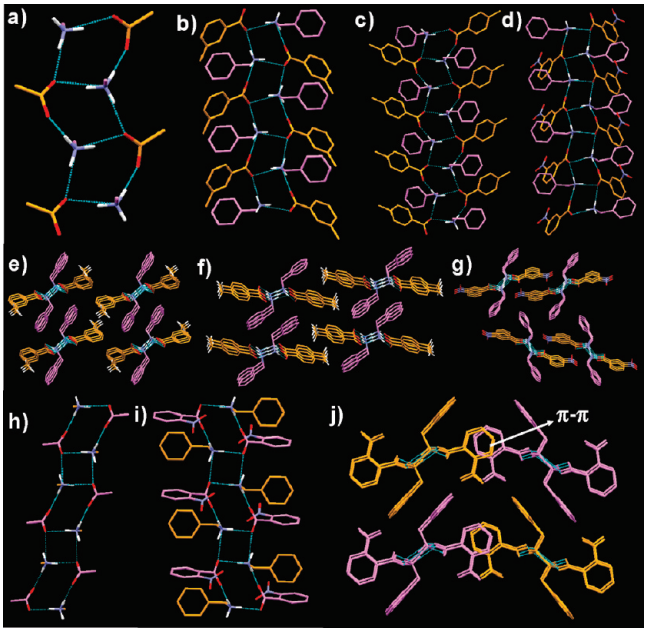

FIGURE 5. Crystal structure illustrations: (a) 1D supramolecular synthon observed in the gelator salts **BA3MB**, **BA4MB**, and **BA3NB**; 1D hydrogen bonded chains present in (b) **BA3MB**, (c) **BA4MB**, (d) **BA3NB**; (e−g) parallel packing of the of the 1D hydrogen bonded chains in **BA3MB**, **BA4MB**, and **BA3NB**, respectively; (h) 1D supramolecular synthon observed in the nongelator salt **BA2NB**; (i) 1D hydrogen bonded chain in **BA2NB**; (j) parallel packing of the 1D hydrogen bonded chains in **BA2NB** displaying $\pi-\pi$ stacking; crystallographic figures for the salt **BA4MB** were generated by using the CIF (Refcode PEBCUV) submitted in the CSD.

Conclusions

The Supramolecular synthon approach has been demonstrated to be a powerful tool to design a new class of gelator derived from a series of benzylammonium benzoate salts. In particular the **PAM** synthon has been exploited in these salts and it is remarkable that 75% of the salts prepared are gelators. Substituents at the 4-position of the anionic moiety gave a maximum number of gelators followed by substituents at the 2- and 3-positions. The majority of the gelator salts showed instant gelation abilities at room temperature, which is technologically important for real-life applications. Single crystal X-ray diffraction studies showed that out of the 5 crystal structures of the gelators, 3 salts displayed 1D and 2 salts displayed 2D synthons emphasizing the importance of 1D as well as 2D HBN in gelation. It is important to note that the most frequently observed **PAM** synthon (synthon X, Scheme 3) is found in the gelator salts that dispayed 1D HBN. XRPD studies revealed that the gel fibers in the xerogels are of different and/or a mixture of various other crystalline phases along with the one represented by the single crystal structures of the gelators.

Although 1D HBN is an important prerequisite for gelation, it is not enough to ensure gel formation. A detailed understanding of the various other parameters that controls gel formation such as nucleation of gel fiber formation, self-assembly of the gel fibers to form SAFIN, interactions of the SAFINs with the targeted solvents to immobilize the solvents (gel formation) are some of the important events need be addressed with great detail before a better strategy of designing LMOGs can be established. The work presented here clearly demonstrates the advantage of the supramolecular approach in synthesizing LMOGs and provides further support to the working hypothesis of rational design of gelators.

Experimental Section

Materials and Physical Measurements. All the reagents were obtained from various commercial sources (Sigma-Alrdrich, S. D. Fine etc.) and used as such without further purification. Solvents were of L. R. grade and were used without further distillation. Both ^{1}H and ^{13}C NMR were performed on a 300 MHz spectrometer (Bruker Avance, DPX-300). For all other experiments standard 5 mm NMR tubes (Aldrich) were used. Chemical shifts (δ) are reported in parts per million (ppm) relative to D_2O and $CDCl_3$ (Aldrich) residual solvent peaks. IR spectra were obtained on a FT-IR instrument (FTIR-8300, Shimadzu). The elemental compositions of the purified compounds were confirmed by elemental analysis (Perkin-Elmer Precisely, Series-II, CHNO/S Analyzer-2400). Scanning electron microscopy (SEM) was recorded in a JEOL, JMS-6700F, Field Emission Scanning Electro Microscope. Differential Scanning Calorimetry (DSC) was recorded in a Perkin-Elmer, Diamond DSC.

Hazard!! Benzylamine should be handled with caution since inhalation of this compound may cause severe burns to the mucous membrane tissue.

General Synthetic Procedure. All the salts were prepared following the typical procedure. Methanolic solutions of acid and amine were prepared. Then, a solution of the amine was

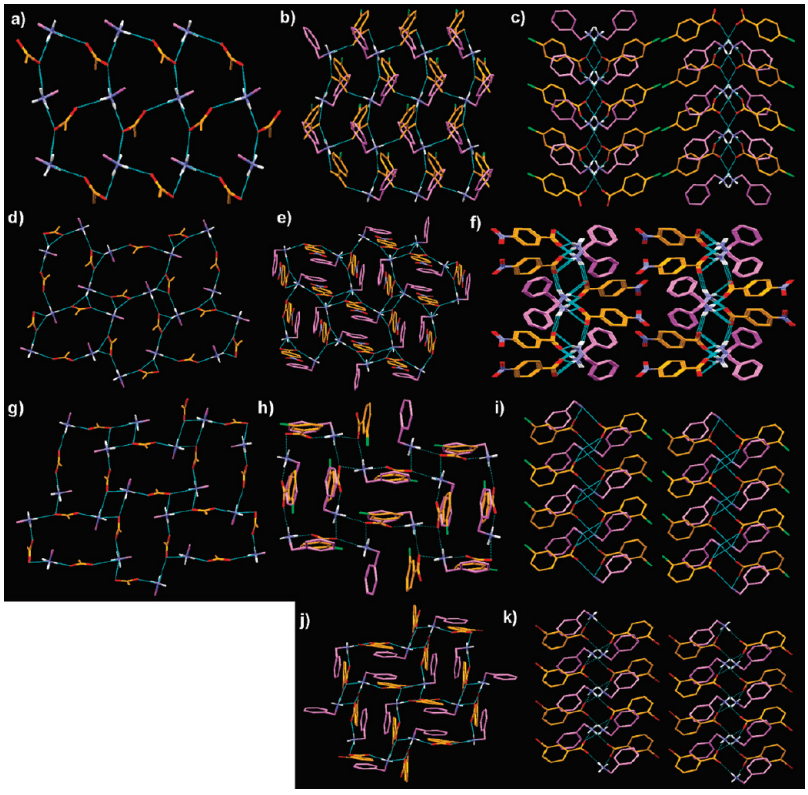

FIGURE 6. Crystal structure illustrations: (a and d) 2D supramolecular synthons obtained in the gelator salts **BA4CB** and **BA4NB**, respectively; (b−c and e−f) 2D hydrogen bonded networks and their parallel packing in the salts **BA4CB** and **BA4NB**, respectively; (g) 2D supramolecular synthon observed in the nongelator salts **BA3CB** and **BA3BB**; (h−i and j−k) 2D hydrogen bonded networks and their parallel packing in the salts **BA3CB** and **BA3BB**, respectively.

added to the solution of the acid and the resulting mixture was kept at room temperature from which a white solid was harvested after 1−2 days in near-quantitative yield and characterized by FT-IR and both ^{1}H and ^{13}C NMR and elemental analyses.

***T*$_{gel}$ Measurements.** In a typical experiment, the salt was dissolved in the targeted solvent by heating. The solution was then allowed to cool to room temperature. Gel formation was confirmed by tube inversion. T_{gel} was measured by the dropping ball method; a glass ball weighing 222.0 mg was placed on a 0.5 mL gel taken in a test tube (10 mm × 100 mm). The tube was then immersed in an oil bath placed on a magnetic stirrer in order to ensure uniform heating. The temperature was noted when the ball touched the bottom of the tube.

BA2MB: mp 130−132 °C. Elemental analysis calcd for $C_{15}H_{17}NO_2$: C 74.05, H 7.04, N 5.76. Found: C 74.13, H 6.76, N 5.85. ^{1}H NMR (300 MHz, D_2O) δ 7.36 (s, 5H), 7.227−7.10 (m, 4H), 4.06 (s, 2H), 2.24 (s, 3H). ^{13}C NMR δ 179.09, 139.74, 133.92, 132.60, 130.23, 129.19, 129.17, 128.75, 128.41, 125.97,125.48, 43.07, 19.02. FT-IR (KBr pellet) 2974, 2947, 2900, 2837, 2754, 2640, 2166, 1637, 1581, 1562, 1491, 1458, 1394, 1155, 843, 783, 744, 698 cm^{-1}.

BA3MB: mp 150−153 °C. Elemental analysis calcd for $C_{15}H_{17}NO_2$: C 74.05, H 7.04, N 5.76. Found: C 74.77, H 7.06, N 6.32. ^{1}H NMR (300 MHz, D_2O) δ 7.59−7.25 (m, 9H), 4.06 (s, 2H), 2.27 (s, 3H). ^{13}C NMR δ 138.36, 136.27, 132.69, 131.76, 129.27, 129.15, 129.12, 128.72, 128.20, 125.81, 43.08, 20.40. FT-IR (KBr pellet) 2887, 2798, 2740, 2640, 2428, 2171, 1624, 1595, 1523, 1454, 1386, 1282, 1218, 1167, 1080, 978, 893, 785, 756, 700, 671, 582, 409 cm^{-1}.

BA4MB: mp 161−162 °C. Elemental analysis calcd for $C_{15}H_{17}NO_2$: C 74.05, H 7.04, N 5.76. Found: C 74.07, H 7.05, N 5.72. ^{1}H NMR (300 MHz, D_2O) δ 7.70−7.67(d, J = 9 Hz, 2H), 7.39 (s, 5H), 7.23−7.20 (d, J = 9 Hz, 2H), 4.1 (s, 2H), 2.3 (s, 3H). ^{13}C NMR δ 142.09, 133.22, 132.57, 129.18, 128.98, 128.83, 128.76, 43.07, 20.45. FT-IR (KBr pellet) 2877, 2783, 2738, 2644, 2522, 2430, 2206, 1630, 1585, 1512, 1456, 1375, 1290, 1251, 1219, 1172, 1072, 976, 889, 845, 761, 698, 611, 582, 519 cm^{-1}.

BA2CB: mp 151−152 °C. Elemental analysis calcd for $C_{14}H_{14}ClNO_2$: C 63.76, H 5.35, N 5.31. Found: C 63.96, H 5.21, N 5.22. ^{1}H NMR (300 MHz, D_2O) δ 7.37−7.22 (m, 9H), 4.07 (s, 2H). ^{13}C NMR δ 175.87, 139.08, 132.62, 129.55, 129.43, 129.19, 129.17, 43.09. FT-IR (KBr pellet) 3003, 2970, 2904, 2750, 2646, 2166, 1639, 1583, 1497, 1462, 1433, 1394, 1215, 1155, 1051, 1030, 839, 767, 748, 715, 698, 650, 580, 486, 451 cm^{-1}.

BA3CB: mp 147−149 °C. Elemental analysis calcd for $C_{14}H_{14}ClNO_2$: C 63.76, H 5.35, N 5.31. Found: C 63.69, H 5.06, N 5.55. ^{1}H NMR (300 MHz, D_2O) δ 7.71 (s, 1H), 7.65−7.62 (d, J = 9 Hz, 1H), 7.43−7.28 (m, 7H), 4.06 (s, 2H). ^{13}C NMR δ 138.36, 133.59, 132.70, 130.96, 129.83, 129.27, 128.85, 128.74, 127.12, 43.19. FT-IR (KBr pellet) 3064, 3014, 2998, 2912, 2717, 2613, 2521, 1632, 1589, 1551, 1508, 1454, 1387, 1308, 1290, 1213, 1067, 866, 756, 731, 698, 675, 577, 490 cm^{-1}.

BA4CB: mp 157−158 °C. Elemental analysis calcd for $C_{14}H_{14}ClNO_2$: C 63.76, H 5.35, N 5.31. Found: C 63.82, H 5.15, N 5.27. ^{1}H NMR (300 MHz, D_2O) δ 7.71−7.69 (d, J = 6 Hz, 2H), 7.37−7.34 (7H, m), 4.07 (s, 2H). ^{13}C NMR δ 136.54, 134.77, 132.56, 130.34, 129.18, 128.76, 128.23, 43.09. FT-IR (KBr pellet) 3033, 2951, 2883, 2781, 2744, 2648, 2519, 2143, 1632, 1589, 1545, 1531, 1454, 1387, 1309, 1286, 1213, 1161, 1089, 1008, 972, 835, 779, 752, 702, 590, 523 cm^{-1}.

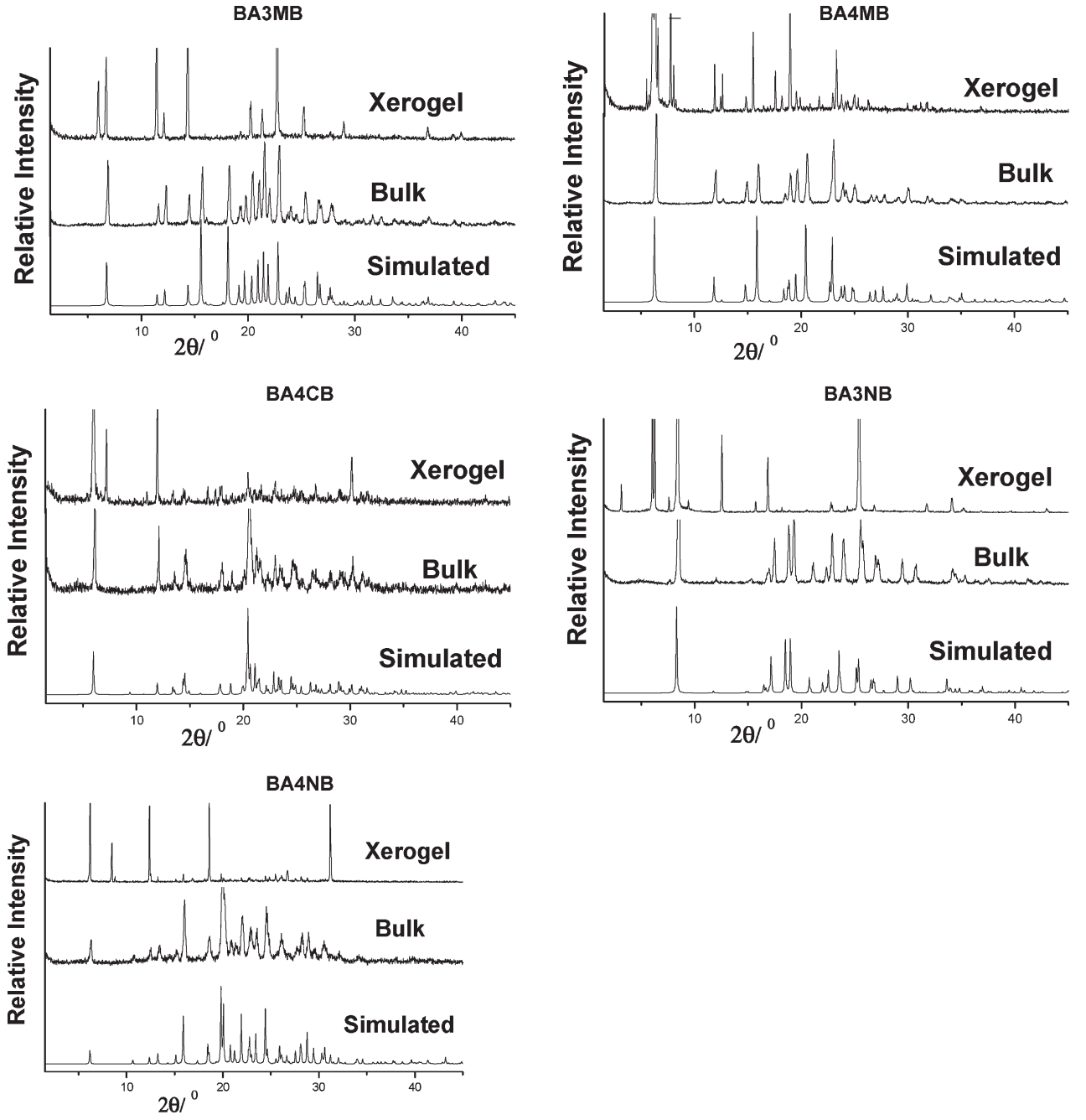

FIGURE 7. XRPD patterns of the gelator salts under various conditions.

BA2BB: mp 152−154 °C. Elemental analysis calcd for $C_{14}H_{14}BrNO_2$: C 54.56, H 4.58, N 4.55. Found: C 55.14, H 4.42, N 4.82. ^{1}H NMR (300 MHz, $CDCl_3$) δ 7.49−7.46 (d, J = 9 Hz, 1H), 7.29−7.23 (m, 8H), 3.9 (s, 2H). ^{13}C NMR (D_2O) δ 141.63, 132.65, 132.59, 129.67, 129.29, 128.86, 127.57, 127.05, 117.09, 43.16. FT-IR (KBr pellet) 3003, 2970, 2901, 2746, 2644, 2540, 2162, 1637, 1583, 1495, 1460, 1429, 1392, 1288, 1255, 1215, 1155, 1026, 837, 767, 746, 696, 644, 414 cm^{-1}.

BA3BB: mp 153−154 °C. Elemental analysis calcd for $C_{14}H_{14}BrNO_2$: C 54.56, H 4.58, N 4.55. Found: C 54.63, H 4.32, N 4.69. ^{1}H NMR (300 MHz, D_2O) δ 7.87 (s, 1H), 7.69−7.66 (d, J = 9 Hz, 1H), 7.57−7.54 (d, J = 9 Hz, 1H), 7.34−7.21 (m, 6H), 4.05 (s, 2H). ^{13}C NMR δ 138.48, 133.79, 132.83, 131.62, 130.01, 129.16, 129.1, 128.70, 128.43, 127.45, 121.62, 43.13. FT-IR (KBr pellet) 3063, 3014, 2991, 2910, 1632, 1589, 1549, 1446, 1387, 1209, 1142, 1065, 893, 858, 754, 698, 569 cm^{-1}.

BA4BB: mp 160−162 °C. Elemental analysis calcd for $C_{14}H_{14}BrNO_2$: C 54.56, H 4.58, N 4.55. Found: C 54.32, H 4.57, N 4.42. ^{1}H NMR (300 MHz, D_2O) δ 7.67−7.64 (d, J = 9 Hz, 2H), 7.55−7.53 (d, J = 6 Hz, 2H), 7.38 (s, 5H), 4.09 (s, 2H). ^{13}C NMR δ 135.08, 132.60, 131.23, 130.54, 129.17, 129.16, 128.74, 125.06, 43.09. FT-IR (KBr pellet) 2887, 2744, 2648, 2522, 2141, 1634, 1587, 1543, 1456, 1387, 1304, 1163, 1067, 1011, 833, 775, 750, 700, 471 cm^{-1}.

BA2NB: mp 150−151 °C. Elemental analysis calcd for $C_{14}H_{14}N_2O_4$: C 61.31, H 5.14, N 10.21. Found: C 61.11, H 5.13, N 10.31. ^{1}H NMR (300 MHz, D_2O) δ 8.00−7.97 (d, J = 9 Hz, 1H), 7.68−7.63 (t, J = 9 Hz, 1H), 7.49−7.44 (m, 7H), 4.08 (s, 2H). ^{13}C NMR δ 174.78, 144.44, 135.77, 134.69, 132.62,

129.18, 129.03, 128.75, 127.38, 124.04, 43.08. FT-IR (KBr pellet) 3016, 2905, 2820, 2719, 2642, 2424, 1630, 1560, 1516, 1472, 1458, 1439, 1381, 1348, 1311, 1261, 1144, 1070, 789, 748, 689, 420 cm^{-1}.

BA3NB: mp 180−182 °C. Elemental analysis calcd for $C_{14}H_{14}N_2O_4$: C 61.31, H 5.14, N 10.21. Found: C 61.28, H 5.05, N 10.62. ^1H NMR (300 MHz, D_2O) δ 8.52 (s, 1H), 8.25−8.22 (d, J = 9 Hz, 1H), 8.12−8.09 (d, J = 9 Hz, 1H), 7.59−7.53 (t, J = 9 Hz, 1H), 7.36 (s, 5H), 4.08 (s, 2H). ^{13}C NMR δ 138.01, 135.06, 129.45, 129.14, 129.12, 128.72, 125.57, 123.55, 43.08. FT-IR (KBr pellet) 2943, 2893, 2746, 2660, 2428, 1632, 1589, 1545, 1522, 1427, 1371, 1346, 1213, 1159, 1068, 964, 823, 814, 764, 721, 698 cm^{-1}.

BA4NB: mp 195−196 °C. Elemental analysis calcd for $C_{14}H_{14}N_2O_4$: C 61.31, H 5.14, N 10.21. Found: C 61.40, H 5.05, N 10.39. ^1H NMR (300 MHz, D_2O) δ 8.19−8.16 (d, J = 9 Hz, 2H), 8.00−7.87 (d, J = 9 Hz, 2H), 7.37 (s, 5H), 4.09 (s, 2H). ^{13}C NMR δ 142.71, 129.52, 129.15, 128.729, 123.44, 43.09. FT-IR (KBr pellet) 3032, 2910, 2733, 2692, 2118, 1636, 1618, 1573, 1516, 1454, 1389, 1344, 1213, 1132, 1103, 881, 825, 798, 758, 725, 700, 577, 507 cm^{-1}.

Acknowledgment. U.K.D. thanks CSIR, New Delhi for a Junior Research Fellowship (JRF). A.N.N. thanks IACS for a Senior Research Fellowship (SRF). Some of the single crystal X-ray diffraction data were collected at the DST-funded National Single Crystal Diffractometer facility at the Department of Inorganic Chemistry, IACS, Kolkata.

Supporting Information Available: Crystallographic parameter table, molecular plots with atom numbering scheme, hydrogen bonding parameters, ^1H and ^{13}C NMR spectra, and CIF files. This material is available free of charge via the Internet at http://pubs.acs.org.